

Continuous-flow electrophoresis in the Taylor regime: a new possibility for preparative electrophoresis

Michael J. Clifton

Laboratoire de Génie Chimique (CNRS UMR 5503), Université Paul Sabatier, 118 Route de Narbonne, 31062 Toulouse cedex, France

Received 10 April 1996; revised 19 June 1996; accepted 24 July 1996

Abstract

A theoretical and numerical analysis shows that by performing continuous-flow electrophoresis in a chamber with a thickness of about 0.2 mm, most of the effects that cause spreading of protein filaments can be suppressed and the convective spreading is replaced by less extensive Taylor dispersion. An expression is derived that gives the resolution of the system as a function of the various design parameters. The optimum values for these parameters have been identified. Proteins with a mobility differing by only 10% can be completely separated and the sample treatment rate is of the order of 1 ml/h.

Keywords: Taylor dispersion; Continuous-flow electrophoresis; Preparative electrophoresis

1. Introduction

The need for a new high-performance preparative technique in the separation of biological molecules, such as proteins, is becoming more and more apparent. This is demonstrated by the increasingly common presentation of gel and capillary electrophoresis as “micro-preparative” processes. Though a number of preparative techniques based on electrophoresis already exist [1–5], continuous-flow electrophoresis offers several advantages that are not always found in other processes: separation based on mobility differences, continuous rather than batch operation, little contact with solid surfaces (so little denaturing). These qualities and some applications of the process have been explained in detail in two recent reviews [6,7]. However continuous-flow electrophoresis (CFE) is also plagued by the presence of a number of secondary phenomena that interfere with separation and reduce resolution [8]: non-uniform residence times, electro-osmosis, electrohydrodynamics

and electrokinetic spreading. The general tendency in solving these problems has been to use thicker chambers and well centred injection to reduce wall effects, i.e., the “crescent” effect due to non-uniform residence times and electro-osmosis. However this amplifies the disturbances caused by natural convection due to mass transfer at the electrodes and non-uniform Joule heating [9]. Though the latter problem is of little importance for an electrophoresis chamber operated in microgravity, the electrohydrodynamic spreading is still present [10] and microgravity is hardly a solution for everyday separations.

On the other hand, a solution to these problems may lie in the use of a very thin chamber. Taylor [11] has developed a formula giving the axial dispersion by convection and diffusion of a narrow band of solute flowing through a fine tube. This expression can be adapted to the geometry of a CFE chamber. It is then found that for sufficiently thin chambers, the convective-diffusive spreading (that corresponds to the “crescent” effect) can be kept to

quite low levels. In such a geometry, other secondary effects that degrade separation in CFE, electrohydrodynamics and natural convection, are eliminated. Only the electrokinetic spreading – due to non-uniform pH and field strength – remains and this can be minimised by using more concentrated buffers than are acceptable with thick chambers: in such a thin chamber the removal of heat generated by the Joule effect is relatively easy.

2. Theory

The principle of CFE is represented in Fig. 1. A carrier buffer solution is made to flow at a low velocity through a thin rectangular chamber. Electrode compartments on either side of the chamber are used to apply an electric field across its width. The solution containing the protein mixture to be separated is injected into this flow at the entrance of the chamber. The bio-molecules are carried along the chamber by the flow and migrate under the influence of the electric field. As each protein species has a characteristic mobility at the pH fixed by the buffer, the single original filament divides into separate filaments: one for each species. At the outlet of the chamber, the various filaments can be collected separately.

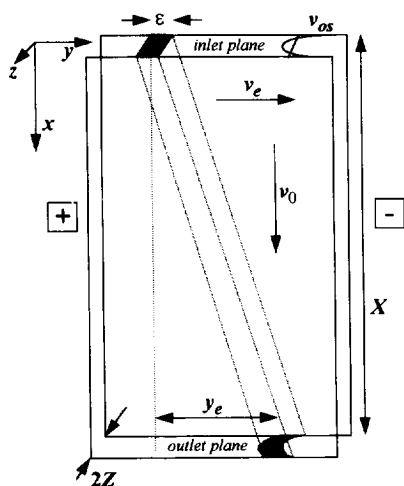


Fig. 1. Continuous-flow electrophoresis: principle of the process, showing the deformation of a protein filament by the effect of convection and migration ("crescent" effect).

To describe this system, we shall limit our treatment to a relatively simple model similar to that of Grateful and Lightfoot [12]. It takes into account the transfer by molecular diffusion, the uniform and independent migration of each species, the imposed laminar (Poiseuille) convection of the carrier solution and its electro-osmotic convection. Dispersion by the "crescent" effect is thus taken into account: this term covers two contributions. In the first of them, the parabolic profile of flow through the chamber implies that molecules near the centre plane of the chamber spend less time in the electric field than those nearer the walls: so the molecules closer to the wall migrate further. The second contribution, electro-osmosis, arises from the fact that the chamber walls carry fixed electrical charges that are neutralised by mobile ionic charges of the buffer. Under the influence of the electric field, the ions in this double layer migrate in the direction of the field and drag water along with them, thus creating a slip velocity at the wall. As the sides of the chamber are closed off by the electrode compartments, the overall result is the formation of a flow pattern in the buffer with a parabolic profile across the chamber thickness and a non-zero velocity at the wall. It has been known for some time that these two phenomena produce a geometrically equivalent distortion of the sample filament and that they can cancel each other out when the electro-osmotic velocity at the wall is equal and opposite to the protein migration velocity [13]. The overall spreading, known as "crescent" dispersion, will be particularly important in the following discussion. However we shall neglect effects such as electrohydrodynamics and natural convection, that should be negligible in thin chamber geometries. Also, to simplify the discussion, the non-uniformities of field strength and pH and the associated interactions between the migrating species will not be considered.

Under conditions where the above assumptions apply, the system arrives rapidly at a steady state that can be represented by the following diffusion-convection equation, giving the concentration c of the species considered:

$$v_x \frac{\partial c}{\partial x} + v_y \frac{\partial c}{\partial y} = D \left(\frac{\partial^2 c}{\partial y^2} + \frac{\partial^2 c}{\partial z^2} \right) \quad (1)$$

where the x -axis is in the direction of carrier flow, y

in the field direction and z perpendicular to the chamber walls. It should be noted that the diffusive transport in the x direction has been supposed negligible. Here D is the diffusion coefficient and the velocity components v_x and v_y include the migration velocity together with the strictly convective velocities:

$$v_x = v_0 \frac{3}{2} \left[1 - \left(\frac{z}{Z} \right)^2 \right] \tag{2}$$

where v_0 is the mean carrier velocity and Z is the chamber half-thickness.

$$v_y = v_e + \frac{v_{os}}{2} \left[3 \left(\frac{z}{Z} \right)^2 - 1 \right] \tag{3}$$

where v_e is the migration velocity and v_{os} the electro-osmotic slip velocity at the wall. The boundary conditions for Eq. (1) are: (a) $\partial c / \partial z = 0$ for $z = 0, \pm Z$; (b) $c = 0$ for $y = \pm \infty$; (c) at $x = 0$: $c = c_0$ for $-\varepsilon/2 \leq y \leq +\varepsilon/2$ and $c = 0$ for $y < -\varepsilon/2$ and $y > +\varepsilon/2$; (d) $c \rightarrow 0$ for $x \rightarrow \infty$ where ε is the width of the initial band of concentration c_0 . It should be noted that the injection zone is extended across the whole chamber thickness: this is not the usual practice with thick chambers but this distribution has been adopted here in all cases to facilitate comparison between the different geometries. The analysis will in any case insist mainly on thin chamber geometries.

It is useful to define a new set of axes:

$$x_1 = x/Z \quad y_1 = (y + ax)/Z \quad z_1 = z/Z \tag{4}$$

where the constant a has yet to be defined.

In terms of these axes Eq. (1) takes on the following form:

$$\frac{Zv_x}{D} \frac{\partial c}{\partial x_1} + \frac{Z(av_x + v_y)}{D} \frac{\partial c}{\partial y_1} = \frac{\partial^2 c}{\partial y_1^2} + \frac{\partial^2 c}{\partial z_1^2} \tag{5}$$

The velocity v_1 is then defined as:

$$v_1 = av_x + v_y \\ = v_e + \frac{1}{2}(3av_0 - v_{os}) - \frac{3}{2}(av_0 - v_{os})z_1^2 \tag{6}$$

From Eq. (6), the value for a can be chosen in various ways, but to follow the treatment by Taylor the mean velocity in the y_1 direction must be zero:

$$\int_0^1 v_1 dz_1 = v_e + av_0 = 0 \tag{7}$$

So $a = -v_e/v_0$ and the velocity v_1 is given by:

$$v_1 = \frac{1}{2}(v_e + v_{os})(3z_1^2 - 1) \tag{8}$$

The band distortion created by this velocity distribution will give rise to a molecular diffusion flux in the z direction that will tend to recreate a uniform concentration distribution in this direction: this is illustrated in Fig. 2. This mechanism will be particularly effective for thin chambers for which $Z \ll \varepsilon$. In this case, we can assume that $\partial^2 c / \partial y_1^2 \ll \partial^2 c / \partial z_1^2$. Furthermore, we shall consider the transfer through a plane given by a constant value for y_1 ; on such a plane the concentration gradient in the flow direction $\partial c / \partial x_1$ is small and Eq. (5) becomes:

$$\frac{Zv_1}{D} \frac{\partial c}{\partial y_1} = \frac{\partial^2 c}{\partial z_1^2} \tag{9}$$

There is a solution to this equation in the following form:

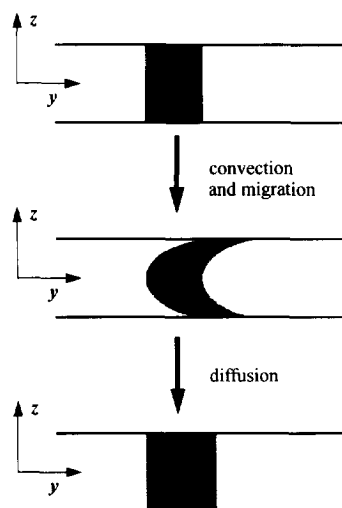


Fig. 2. The mechanism of Taylor dispersion in CFE can be thought of as occurring in two steps. First the filament cross-section is deformed by the "crescent" effect. Then diffusion eliminates concentration gradients in the z direction and there is an overall broadening of the filament. In fact both processes occur simultaneously.

$$c = c_1 + A \left(z_1^2 - \frac{1}{2} z_1^4 \right) \quad (10)$$

where $c_1(x_1, y_1)$ is the concentration in the central plane of the chamber, where $z_1 = 0$. Substituting Eq. (10) in Eq. (9), it is found that:

$$A = - \frac{Z(v_e + v_{os})}{4D} \frac{\partial c_1}{\partial y_1} \quad (11)$$

The mean flux of solute through any y_1 plane at the height x_1 is

$$J = \int_0^1 v_1 c \, dz_1 = - \frac{2}{105} \frac{Z^2(v_e + v_{os})^2}{D} \frac{\partial c_1}{\partial y_1} \quad (12)$$

By analogy with Fick's law of diffusion, the factor that multiplies the concentration gradient can be considered as a diffusion coefficient. This coefficient for convective dispersion in the Taylor regime can be defined as:

$$D_T = \frac{2}{105} \frac{Z^2(v_e + v_{os})^2}{D} \quad (13)$$

It is interesting to note that this dispersion coefficient increases strongly with Z (i.e., with chamber thickness), while paradoxically it decreases with increasing D .

To characterise the quality of separation in an electrophoresis process, the concepts of theoretical plate height, number of theoretical plates and resolution are often used [14]. The theoretical plate height H is defined as the ratio of the variance σ^2 of an approximately Gaussian peak to the migration distance. For a Gaussian peak undergoing diffusion the variance is proportional to the diffusion coefficient and to the time, the appropriate time here being the mean residence time in the chamber ($\tau = X/v_0$):

$$\sigma^2 = 2D^* \tau = 2D^* X/v_0 \quad (14)$$

where X is the chamber length. Here the diffusivity D^* is a generalised diffusion coefficient that can cover phenomena such as molecular diffusion or Taylor dispersion.

As the migration distance y_e is given by the product of the migration velocity and the residence time (τv_e), the height of a theoretical plate is given by:

$$H = \frac{\sigma^2}{y_e} = \frac{2D^*}{v_e} \quad (15)$$

The number of theoretical plates N is the ratio of migration distance to plate height:

$$N = \frac{y_e}{H} = \frac{\tau v_e^2}{2D^*} \quad (16)$$

The resolution of two peaks is given by the distance between their centres $\tau \Delta v_e$ divided by 4σ , where σ is the standard deviation of both peaks, assumed to be equal:

$$R = \frac{\tau \Delta v_e}{4\sigma} = \frac{\Delta u}{4\bar{u}} \sqrt{N} \quad (17)$$

where Δu is the difference in electrophoretic mobility between the two species and \bar{u} is the mean mobility. The condition for complete separation of the two peaks can be taken as $R \geq 1$. To reach this condition, the following condition applies:

$$\frac{\Delta u}{\bar{u}} \geq \frac{4}{\sqrt{N}} = \frac{4\sigma}{\tau v_e} \quad (18)$$

The left-hand side of this inequality can be considered as representing the requirement imposed by the user (a certain fractional difference in mobility between two species that must be separated), whereas the right-hand side represents the limit imposed by the response of the apparatus or the technique used.

In a chamber where the peak broadening is dominated by Taylor dispersion, the diffusivity D^* in Eq. (15) should be replaced by D_T and Eq. (18) becomes:

$$\frac{\Delta u}{\bar{u}} \geq \frac{8}{105} \left(1 + \frac{v_{os}}{v_e} \right) Z \sqrt{\frac{v_0}{DX}} \quad (19)$$

It is worth noting that this expression contains the following dimensionless group, which is the ratio of the chamber half-thickness to the characteristic diffusion length $\sqrt{D\tau}$:

$$T = Z \sqrt{\frac{v_0}{DX}} = \frac{Z}{\sqrt{D\tau}} \quad (20)$$

This quantity is often used to characterise flow with mass transfer [15]: a flow for which $T < 1$ is said to be in the Taylor regime. In this case the

residence time in the channel can be considered sufficiently long for solute to have been able to diffuse from the centre-line to the wall.

If the dispersion is limited to molecular diffusion Eq. (18) becomes:

$$\frac{\Delta u}{u} \geq \frac{4}{v_e} \sqrt{\frac{2Dv_0}{X}} \quad (21)$$

Here a different dimensionless group appears that is the ratio of the characteristic diffusion length to the migration distance:

$$G = \frac{1}{v_e} \sqrt{\frac{2Dv_0}{X}} = \frac{\sqrt{2D\tau}}{v_e\tau} \quad (22)$$

In the case where several different dispersion mechanisms are active, it is common to consider that the overall variance is the sum of the variances due to each mechanism [16]. So, if both Taylor dispersion and molecular diffusion are important, we have:

$$\sigma^2 = 2D\tau + 2D_T\tau + A_0\varepsilon^2 \quad (23)$$

where the last term takes into account the initial width ε of the solute zone and A_0 is a constant that depends on the shape of the initial concentration distribution.

When this more general formula for σ is substituted into Eq. (18), the following expression is obtained:

$$\frac{\Delta u}{u} \geq \sqrt{A_1G^2 + A_2(1+r'_{os})^2T^2 + \frac{A^3}{n^2}} \quad (24)$$

where $r'_{os} = v_{os}/v_e$ is the ratio of the electro-osmotic to the electrophoretic velocities and the coefficients A_1 , A_2 and A_3 replace the various numerical constants that have been encountered. The quantity n is the number of initial zone widths through which the solute has migrated at the chamber outlet:

$$n = \frac{v_e X}{v_0 \varepsilon} = \frac{y_e}{\varepsilon} \quad (25)$$

3. Numerical simulation

To test the hypotheses that have been made up to this point, a numerical solution to Eqs. (1–3) has been studied. The axes of Eq. (4) were used to put

the equations into the form of Eqs. (5,8) and the resulting expression was discretised using a particular finite-difference technique. The diffusion term was represented in a semi-implicit manner while the convection term was represented by a fourth-order explicit technique to keep numerical diffusion at an acceptable level.

To present the results of these calculations, they are expressed in a dimensionless form: this reduces (somewhat) the number of parameters and allows the results to be more easily generalised. The result of interest is the width of the solute band at the chamber outlet. The seven parameters that control this result are: X , v_e , v_{os} , v_0 , ε , D and Z . As these involve only two basic quantities, length and time, the seven dimensioned parameters will be replaced by five dimensionless ones. A dimensional analysis shows that the system is satisfactorily defined by the dimensionless parameters introduced above: T , G , n and r'_{os} , together with the aspect ratio X/Z . The calculations were all performed with a diffusion coefficient D of 6×10^{-11} m²/s: this is a typical value for a protein.

The first result illustrates the transition from the regime of convective spreading to that of Taylor dispersion. Fig. 3 shows the concentration distribution at the chamber outlet obtained for three similar parameter sets: only the chamber half-thickness Z is varied. It can be seen that for the thickest chamber ($2Z=3$ mm, $T=3.87$), the form of the peak is not at all symmetrical: the band has an advancing edge that would contaminate any more mobile proteins. The maximum of the peak has migrated only through 12.9 mm (while $n=15$): this is due to the fact that part of the protein has only experienced the residence time ($2\tau/3$) in the centre plane of the chamber where the laminar flow profile has its maximum. The second profile is for a somewhat thinner chamber ($2Z=1.6$ mm, $T=2.07$): here the edge of the protein band is less widely spread but a tendency appears for the formation of a double peak, corresponding to two different residence times. As a result, the maximum concentration is relatively low in this case. The third profile is for a quite thin chamber ($2Z=0.2$ mm, $T=0.26$) and in this case the mass transfer is within the Taylor regime. The peak has now become Gaussian in shape and the maximum is found at 15 mm, in agreement with the value for n . The peak

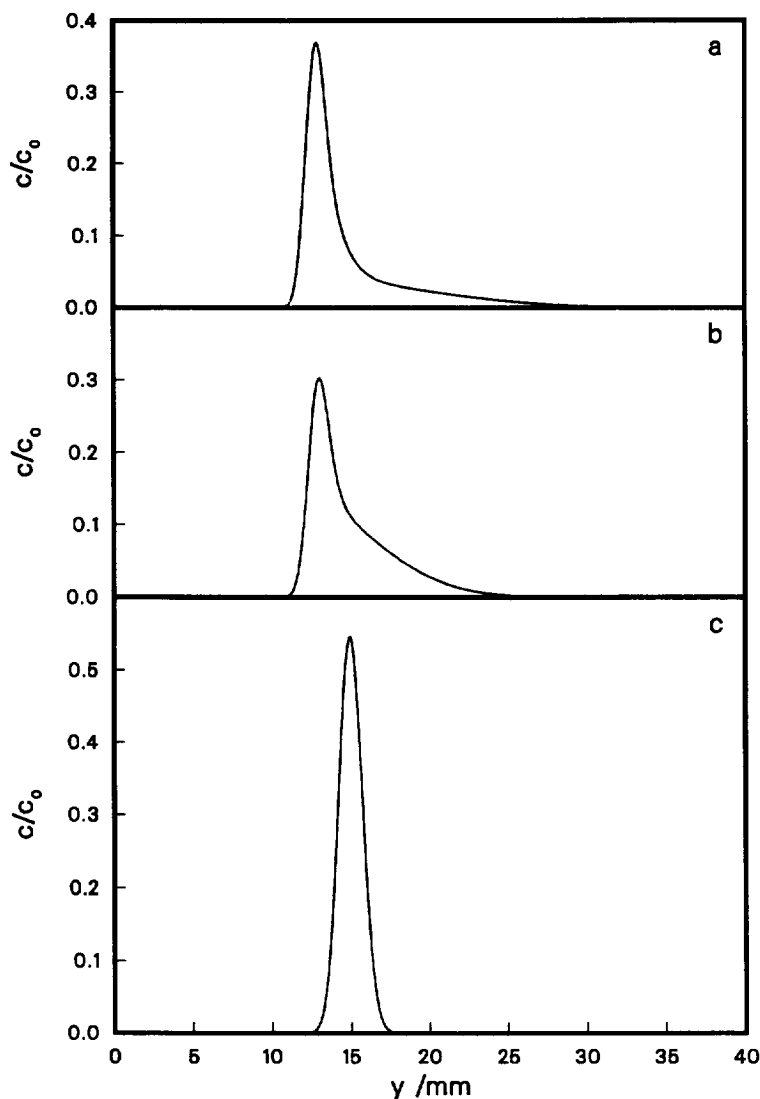


Fig. 3. Calculated concentration distribution at the chamber outlet for different values of the chamber thickness. (a) $2Z=3$ mm, $T=3.87$; (b) $2Z=1.6$ mm, $T=2.07$; (c) $2Z=0.2$ mm, $T=0.26$. Other parameters are: $X=500$ mm; $v_0=0.2$ mm/s; $v_e=6$ $\mu\text{m/s}$; $v_{os}=-3$ $\mu\text{m/s}$; $\varepsilon=1$ mm; $D=6\times 10^{-11}$ m^2/s .

shows little spreading and as a result, the maximum in concentration is much higher.

Next, the simulation was performed for different values of the input parameters. The following values were kept constant: $X=500$ mm, $Z=0.1$ mm, $\varepsilon=1$ mm and $D=6\times 10^{-11}$ m^2/s . The value of X was chosen simply to have a chamber of a reasonable length: in fact the performance of the chamber increases monotonically with X and the limit on this

parameter will be purely technological. The value of Z was chosen sufficiently small so as to remain always within the Taylor regime. The initial zone width ε was also fixed at a small, but technologically realistic, value. The other parameters v_0 , v_e and v_{os} were varied so as to cover a range of values of T and n , while keeping r_{os} at a typical value of -0.5 . This corresponds to varying the field strength and the carrier flow-rate, while operating with a given

chamber geometry and a given solute. The quality of the separation can in fact be judged from the behaviour of a single solute, as can be seen from Eq. (18): this assumes that the two solutes being separated are similar in properties (u and D) and in initial concentration (c_0).

The results of these calculations are shown in Fig. 4. The curves show how the limiting value of $\Delta u/\bar{u}$ varies with n for four values of T . It can be seen that the quality of separation improves as the migration distance n increases: for low n , the value of $\Delta u/\bar{u}$ decreases rapidly showing that smaller and smaller differences in mobility can be resolved, then beyond a certain value for n , little improvement is seen. The asymptotic value of $\Delta u/\bar{u}$, attained at high values of n , decreases with T ; at the same time, for lower values of T a higher value of n is required to approach this asymptotic value of $\Delta u/\bar{u}$.

This behaviour is in agreement with Eq. (24). The contribution from G is relatively small and for a given value of T there is a hyperbolic decrease in $\Delta u/\bar{u}$ with n . The asymptotic limit for high values of n is fixed by T (or by G at very low values of T).

As has been pointed out by many previous authors the ideal value for r_{os} is -1.0 : this corresponds to the case where the protein to be separated has the same zeta potential as the chamber wall and there is no crescent spreading [13]. This is illustrated by Fig.

5 which shows the limiting value of $\Delta u/\bar{u}$ as a function of r_{os} for different values of T . As the ideal situation is approached ($r_{os} = -1$) the value of $\Delta u/\bar{u}$ can reach very low levels. Eq. (24) shows that this level is fixed by n and by G .

From these numerical results, a linear regression analysis was used to calculate the constants in Eq. (24). After substitution of these numerically determined constants, Eq. (24) becomes:

$$\frac{\Delta u}{\bar{u}} \geq \sqrt{22.8G^2 + 0.889(1 + r_{os})^2 T^2 + \frac{2.54}{n^2}} \quad (26)$$

4. Discussion

It remains to be considered whether this system is a feasible one and whether it offers a sufficient rate of production. The latter quantity can be represented by the flow-rate for sample injection, q :

$$q = 2Zv_0\varepsilon \quad (27)$$

The system can be optimised by simple inspection of Eq. (26) and the derivatives of its right-hand side with respect to different parameters; this makes it possible, for a given value of q , to determine optimum values of these parameters that minimise the limiting value of $\Delta u/\bar{u}$. The following extra

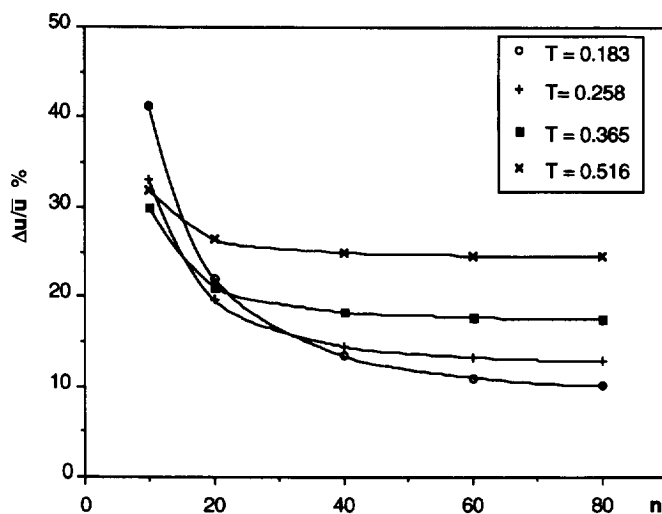


Fig. 4. Limiting value of relative resolution $\Delta u/\bar{u}$ as a function of the dimensionless migration distance n , for various values of the parameter T .

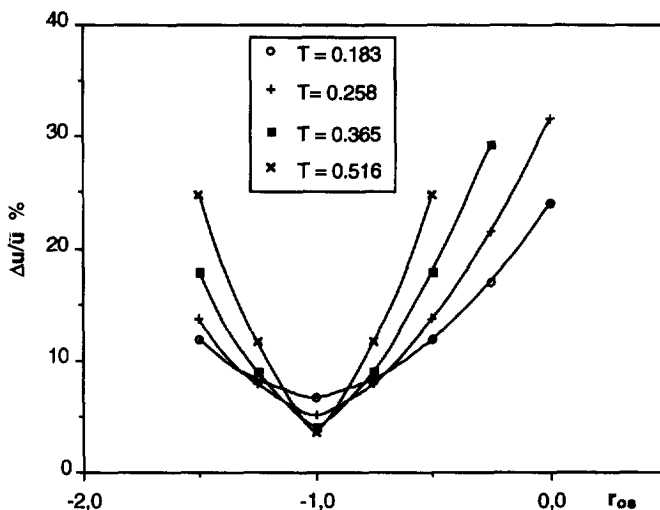


Fig. 5. Limiting value of relative resolution $\Delta u/\bar{u}$ as a function of the ratio r_{os} of electroosmotic velocity to migration velocity, for various values of the parameter T .

constraints were imposed: $r_{os} = -0.5$, $X \leq 600$ mm, $\tau \leq 5400$ s (90 min), $2Z \geq 0.2$ mm, $y_e \leq 300$ mm. The temperature is assumed to be kept constant by a satisfactory cooling system. The constraints on X , Z and y_e are meant to represent technological constraints on chamber dimensions; the values adopted are thought to be realistic, but no serious technological analysis has been performed. A constraint on the residence time (90 min) was adopted even though this process is intended for continuous rather than batchwise operation. This represents the fact that most users would wish to have a fairly short waiting time before the first separated material is recovered: this is to ensure a sufficiently flexible process. In any case, very much longer residence times could encounter problems with pump technology.

The parameters optimised were those on which constraints have been applied. For X and y_e the derivative of the right-hand side of Eq. (26) is always negative so these parameters should be chosen at their maximum values. A relative optimum does exist for Z , but it does not correspond to the optimum for the system and the chamber thickness should really always be minimised. Within the limits imposed, the only useful optimum is that for the residence time. The expression for this optimum value is the following:

$$\tau = \left[\frac{2A_2(1+r_{os})^2 Z^4 X^2 y_e^2}{A_3 q^2 D} \right]^{1/3} \quad (28)$$

It is worth noting that for this value of τ , the second and third terms within the square root of Eq. (26) are equal in value. This means that at this optimum, the spreading due to Taylor dispersion is equivalent to the spreading due to the initial zone width. Table 1 shows values of the optimum τ and the corresponding values of $\Delta u/\bar{u}$ and ε for various values of the injection rate q . As for the other parameters involved in these calculations, X and y_e were fixed at their maximum values and Z at its

Table 1
Optimum residence time (τ) for CFE in Taylor regime with corresponding limiting resolution ($\Delta u/\bar{u}$) and initial zone width (ε) for various injection rates (q)

q (ml/h)	τ (min)	$\Delta u/\bar{u}$ (%)	ε (mm)
0.5	131	8.5	9.1
1.0	83	10.7	11.5
1.5	63	12.2	13.2
2.0	52	13.4	14.5
2.5	45	14.4	15.6
3.0	40	15.3	16.6

Values for other parameters: $2Z=0.2$ mm, $X=600$ mm, $y_e=300$ mm, $r_{os} = -0.5$.

minimum. It can be seen that for the higher injection rates, the optimum residence time is smaller than the maximum value imposed and it gets shorter as the injection rate is increased.

This process of CFE in the Taylor regime is only interesting when $\Delta u/\bar{u}$ is not much greater than 10% (corresponding to 1600 theoretical plates). Under the conditions assumed here, this means a maximum injection rate of about 1.0 ml/h, though the value of $\Delta u/\bar{u}$ only increases slowly with the injection rate. This production rate may seem small but it should be remembered that higher sample concentrations could be used in such thin chambers without creating problems of filament stability or electrohydrodynamics and it might be worth considering whether a stack of such chambers could be operated in parallel to increase throughput. It should also be noted that as the initial zone is fairly wide (~ 10 mm), the fraction collector need not be very refined.

It is possible to make some remarks about how sensitive the performance is to the various constraints that have been imposed. The value of r_{os} is fairly arbitrary and it has already been noted how greatly the performance could be improved if the zeta potential of the chamber walls could be adjusted to suit the molecules being separated. The rate of production at a given resolution is proportional to the product Xy_e , i.e., chamber length multiplied by width, at least in the range of values close to those chosen here. So the exact ratio of width to length is of little importance. For a given residence time, a wider chamber means a proportionally higher field strength if the migration distance is kept proportional to the width; so the applied voltage will increase as the square of the chamber width, but the energy dissipated by Joule heating will remain the same.

There are already CFE chambers commercially available that come close to fulfilling the conditions presented here. These are the Octopus PZE chambers manufactured by Dr. Weber GmbH (Ismaning, Germany). Their chamber gap is 500 μm long, 100 μm wide and 0.5 μm thick [17,18]; they allow a maximum residence time of about 25 min. These quantities give a value of T of about 0.83 for a typical protein. So these chambers can be operated just within the Taylor regime. However this value for T is still quite high and a rapid estimation with Eq. (26), putting r_{os} at -0.5 to simplify comparison

with the earlier calculations, shows that the best resolution that can be achieved under these conditions is a $\Delta u/\bar{u}$ of about 35%. Of course a better separation can be achieved with r_{os} closer to the ideal value of -1.0 , but the same can be said of all chamber geometries. The thickness of these chambers was essentially chosen to limit instabilities in buffer flow due to natural convection [6] and it is these instabilities that limit the residence time. An even thinner chamber would reduce Taylor dispersion (T is reduced) and further stabilise the buffer flow thus allowing longer residence times.

5. Conclusion

Continuous-flow electrophoresis in the Taylor regime offers a new possibility for the use of CFE in protein separation. By using a very thin chamber, spreading due to convective effects ("crescent" effect) is replaced by the less harmful Taylor dispersion; other phenomena that reduce resolution such as electrohydrodynamics and natural convection are virtually suppressed. Though the production rate is not very high, the resolution can be very good. It remains to be seen whether technological constraints will allow chambers with this geometry to be built.

6. Symbols

A_i	constant
c	concentration
c_0	initial sample concentration
D	coefficient for molecular diffusion
D^*	generalised diffusivity
D_T	coefficient for Taylor dispersion
G	$\sqrt{2D}/\tau/v_e$
H	height of a theoretical plate
n	y_e/ε
N	number of theoretical plates
q	sample injection rate
r_{os}	v_{os}/v_e
R	resolution of two solute distributions
T	$Z/\sqrt{D\tau}$
u	electrophoretic mobility
v_e	electrophoretic migration velocity
v_{os}	electro-osmotic velocity at the wall

v_x, v_y	components of flow velocity
v_0	mean carrier velocity
x, y, z	space co-ordinates
x_1, y_1, z_1	dimensionless co-ordinates
X	chamber length
y_c	migration distance
Z	chamber half-thickness
ε	initial zone width
σ	standard deviation of solute distribution
τ	mean residence time (X/v_0)

References

- [1] P.G. Righetti, M. Faupel and E. Wenisch, *Adv. Electrophor.*, 5 (1992) 159–200.
- [2] M. Bier and N.B. Egen, *Dev. Biochem.*, 7 (1979) 35–48.
- [3] N.B. Egen, W. Thormann, G.E. Twitty and M. Bier, *Electrophoresis '83*, Walter de Gruyter, Berlin, 1984, pp. 547–550.
- [4] M. Bier, G.E. Twitty and J.E. Sloan, *J. Chromatogr.*, 470 (1989) 369–376.
- [5] J. Caslavská, P. Gebauer and W. Thormann, *Electrophoresis*, 15 (1994) 1167–1175.
- [6] K. Hannig and H.G. Heidrich, *Free-flow Electrophoresis*, GIT Verlag, Darmstadt, 1990.
- [7] M.C. Roman and P.R. Brown, *Anal. Chem.*, 66 (1994) 86A–94A.
- [8] M.J. Clifton, *Electrophoresis*, 14 (1993) 1284–1291.
- [9] J. Heinrich, M.J. Clifton and H. Wagner, *Int. J. Heat Mass Transfer*, 36 (1993) 3703–3710.
- [10] M.J. Clifton, H. Roux-de Balmann and V. Sanchez, *AIChE J.*, in press.
- [11] G.I. Taylor, *Proc. Roy. Soc. London A*, 219 (1953) 186–203.
- [12] T.M. Grateful and E.N. Lightfoot, *J. Chromatogr.*, 594 (1992) 341–349.
- [13] A. Strickler and T. Sacks, *Ann. N.Y. Acad. Sci.*, 209 (1973) 497–514.
- [14] J.C. Giddings, *Sep. Sci.*, 4 (1969) 181–189.
- [15] R.F. Probstein, *Physicochemical Hydrodynamics: An Introduction*, Butterworths, Boston, 1989.
- [16] R. Kuhn and S. Hoffstetter-Kuhn, *Capillary Electrophoresis: Principles and Practice*, Springer, Berlin, 1993, p. 37.
- [17] B. Bondy, J. Bauer, I. Seuffert and G. Weber, *Electrophoresis*, 16 (1995) 92–97.
- [18] J. Bauer and G. Weber, *Electrophoresis*, 17 (1996) 526–528.